J. Adhesion, 1994, Vol. 44, pp. 69–83
Reprints available directly from the publisher
Photocopying permitted by license only
© 1994 Gordon and Breach Science Publishers S.A.
Printed in the United States of America

Effect of Adhesive Stiffness and Thickness on Stress Distributions in Structural Finger Joints

LESLIE H. GROOM

USDA Forest Service, Southern Forest Experiment Station, Pineville, LA 71360-5500, U.S.A.

and

ROBERT J. LEICHTI

Department of Forest Products, Oregon State University, Corvallis, OR 97331, U.S.A.

(Received March 23, 1993; in final form September 29, 1993)

Environmental, political, and socioeconomic actions over the past several years have resulted in a decreased wood supply at a time when there is an increased demand for forest products. This combination of increased demand and decreased supply has forced more emphasis on engineered wood products, a varied category usually connected with adhesively-bonded end joints, of which the most common type is the finger joint. This paper presents the results of a finite-element analysis of structural finger joints, and focuses primarily on the effect of adhesive stiffness and thickness on stress distribution patterns in finger joints. Results indicate that a flexible adhesive layer concentrates adherend longitudinal and radial stresses at the finger base, whereas a stiff adhesive layer minimizes adherend stresses but increases adhesive stress levels. Results also show that a thin adhesive layer concentrates longitudinal adherend stresses at the juncture of the finger tip and flexible finger base and concentrates radial stresses at all finger bases. However, these increased longitudinal and radial stresses are balanced by reduced adhesive shear stresses.

KEY WORDS Finger joint; stress distribution; finite-element method; longitudinal stress; shear stress; wood; adhesive joints; mechanical analysis; theory.

INTRODUCTION

Public concern over environmental issues has triggered a reevaluation of traditional forestry practices and harvesting methods that will dramatically affect the timber supply in the coming years. Early projections indicate that a smaller volume of timber will be cut and the average age of harvested trees will be younger.[1] This younger timber will contain a greater proportion of juvenile wood to mature wood, resulting in a reduction of the mechanical and physical properties of the future timber supply. Compounding this problem is an expected increase in the worldwide demand for timber.[1] Increasing demand combined with decreasing supply will force more emphasis on engineered wood products.

The idea behind engineered systems is to build structural units or subassemblies from smaller components, thus making more efficient use of available resources. The mechanical behavior of engineered systems is dictated by the performance of the

individual components and the way the components are connected. The adhesive end joint is a common component in almost all engineered wood products. The finger joint is the most common type of adhesive end joint, because of its ease of assembly and production handling. Finger joints have been used in both solid lumber of veneers, and they have reported efficiencies ranging from 50 to 90 percent.[2-7] The efficiency of these joints depends on the mechanical properties of the materials in the finger joints and the way they are joined. It is critical to determine the mechanical behavior of finger joints, as they have been documented as failure locations in engineered wood products.[4,8]

Structural finger joints in wood were developed by empirical investigation of certain processing variables on finger-joint mechanical performance.[2,5,7,9-13] These early studies were quite laborious and focused chiefly on processing variables while ignoring the effect of material properties. Empirical comparisons between adhesive end joints do not show distribution of stresses, constrain alternatives, and yield marginal results because of the inherent variability of wood. Development of analytical finger-joint models contributes to the understanding of stress transfer mechanisms and effects of joint parameters such as geometry and material properties.

Current analytical work on finger-joint stress distributions yields some results seen in early studies on butt joints, which transmit uniaxial loads, and lap joints, which transmit pure shear. Erdogan and Ratwani[14] defined and solved a series of governing differential equations in which the adhesive layer was assumed to act as a combination of shear and tension springs. They found that for stepped joints, shear stresses are concentrated around the step ends, with the greater portion of the load carried by the stiffer material. Sawa *et al.*[15] defined and numerically solved the governing differential equations of a butt joint consisting of two dissimilar tubular shafts subjected to torsional loads. They found that the larger the ratio of the shear modulus of an adhesive to that of the adherends, the larger the singularity of the stress at the inner and outer circumferences of the interface.

Smith and Penney[16] gave reasonable estimates of stress intensity factors for cracks emanating from edge butt joints and embedded butt joints using fracture mechanics equations developed from strain energy principles. They concluded that fracture mechanics methods are applicable to predicting butt joint failure in glulam beams. Chen and Cheng[17] studied stress distributions in lap joints using the two-dimensional elasticity theory in conjunction with the variational principle of complementary energy. They found that a relatively inflexible adhesive layer may lead to unsatisfactory joints because of intensified stresses. Chen and Cheng[18] recently modified this theory to examine scarf and butt joints. They presented a closed-form solution describing expected angles that yield uniform adhesive stresses in joints with identical adherends as well as shear and normal stresses in joints with dissimilar adherends.

One of the most common analytical methods of examining stress distributions in adhesively-bonded joints is the finite-element (FE) method. Reddy and Roy[19] wrote a treatise on the general applicability of the FE method to adhesively-bonded joints. Groth and Brottare[20] used FE models to study the effect of apparent stiffness of a thick adhesive layer in a butt joint for adhesive materials with elastic-plastic material behavior. They found that although the apparent stiffness of the adhesive layer decreases because of plasticity starting at the intersection of the adhesive and the adherend, the

reduction was not noticed below a nominal strain level of 0.5 percent. Schmueser *et al.*,[21] used the FE method to model the effect of an organic paint primer on stress and strain distributions within an adhesively-bonded single-lap-shear joint, with the results providing a qualitative explanation for enhanced strength characteristics. Roberts[22] used FE analysis in conjunction with a two-stage analytical procedure for determining the shear and normal stresses in a variety of adhesive joints. Amijima and Fujii[23] wrote a stress analysis program for adhesively-bonded joints that is based on an elastic FE model and includes effects of thermal expansion of the components. Some analyses have even combined FE stress distribution patterns of adhesive joints with fracture energy[24–26] to quantify local stress concentrations.

Stress distributions in finger joints have only recently been investigated analytically using the FE method. Aicher and Klöck[27,28] modeled five different finger joints with varying finger lengths and slopes. Results showed that normal stresses in the adherends at the base of the fingers range from about 2.8 to 4.2 times the applied stress. Stresses in the adhesive layer act similarly, with the stress level at the tips of the fingers approximately four times that at the centerpoint of the fingers.

A common problem encountered in FE modeling of finger joints is the relatively thin nature of the adhesive layer in comparison with the adherends. This generally results in large aspect ratios which misrepresent actual displacements and stresses. Modern computing capabilities have greatly reduced the impact of large aspect ratios, allowing practical modeling with tens of thousands of elements. Pellicane[29] has recently approached the difficulty of poor aspect ratios not by sheer computing power, but by definition of a special finite element; the "interfacial element". The interfacial element has a thickness of zero, with actual thickness of the glueline taken into account in the element stiffness matrix.

Leichti[30] modeled structural finger joints under tensile loading using the FE method and strength theory. He showed that stress distributions are related to finger joint geometry, with first failure probably occurring in the adhesive or the adhesive-adherend interface at the finger tips at relatively low stress levels. Although the model identified the region of probable first failure, the load capacity of the finger joint could not be determined because of material property limitations.

Similarly, Groom and Leichti[31] modeled structural finger joints with the FE method to investigate the effect of geometry and adherend stiffness on stress distribution patterns. They found, in adherends mismatched with regard to stiffness, that axial stress concentrations reach a maximum at the tips of the stiffer adherend. The mismatched adherends had little effect on the shear stress distributions in either the adhesive or the adherends. This model was later expanded[32] to include the effect of mismatched geometric alignment on stress distribution patterns.

Many models have been analyzed for adhesively bonded joints,[19–21] and more specifically finger joints.[27–35] Results for all these models yield several basic trends: (1) maximum shear and peel stresses are found at or near the boundaries of the joint; (2) stresses are nearly uniform in the middle of the joint; (3) the stiffer adherend carries a greater proportion of the load; and (4) peel and shear stresses intensify when the adhesive is stiff relative to the adherends. Furthermore, greater adhesive stiffness leads to higher axial normal stresses in the adhesive layer.[31,32] In fact, Chen and Cheng[17] concluded that an inflexible adhesive layer detracts from joint strength.

The objective of this paper is to quantify the effects of adhesive stiffness and glueline thickness on stress distribution patterns in structural finger joints. This was accomplished by evaluating a series of FE models that examine the effect of adhesive stiffness over a reasonable range. Then, the FE model was modified to reflect changes in glueline thickness.

FINITE-ELEMENT MODELING PROCEDURES

The basic FE model used in this study, shown in Figure 1, was based on a finger joint traditionally used in structural applications. This model, similar in design to models by Aicher and Klöck,[27,28] Groom and Leichti,[31] Leichti and Groom,[32] and Milner and Yeoh,[33] alleviates the main problem of poor aspect ratios encountered in previous models. The largest aspect ratios of elements near areas of high stress concentrations were approximately 3:1. Although aspect ratios of some elements in this study were approximately 30:1, these elements were in noncritical regions between the tips of the adherends. The finger joint model was subjected to uniaxial tensile loading and solved using ANSYS finite-element software. Finite elements consisted solely of solid, two-dimensional, four-node isoparametric quadrilaterals. The model comprised 7,068 elements and 7,250 nodes.

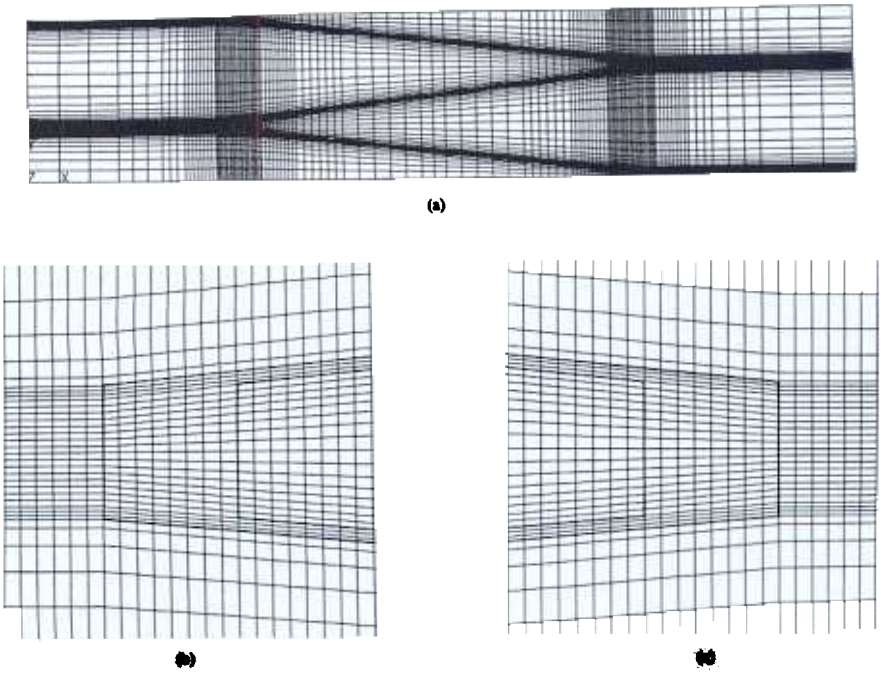

FIGURE 1 Finite element mesh used for adhesive stiffness showing (a) mesh of entire model, (b) mesh closeup of flexible adherend base/stiff adherend tip juncture, and (c) mesh closeup of flexible adherend tip/stiff adherend base juncture.

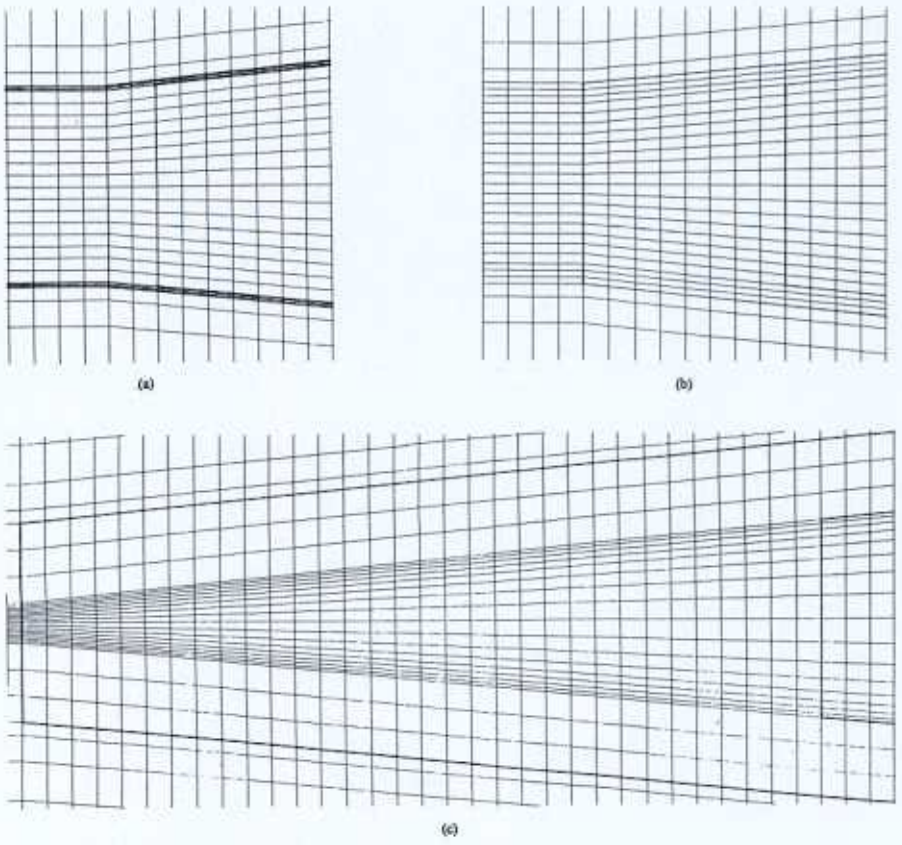

FIGURE 2 Closeup of finite element mesh used to evaluate the effect of adhesive thickness on stress distributions in structural finger joints. The closeups focus on the flexible adherend base/stiff adherend tip juncture for gluelines varying from (a) 0.001 in.; (b) 0.004 in.; and (c) 0.016 in.

Material Properties

The model was composed of three basic material types: left adherend, structural adhesive layer, and right adherend. Material properties for the left and right adherends were chosen to represent wood, which in this study was considered to be homogeneous, orthotropic, and oriented in the longitudinal-radial plane. Stiffness values for the adherends were mismatched such that the longitudinal modulus of elasticity (MOE) of the left adherend was 1.4×10^6 pounds per square inch (psi) (9.6 GPa) and that of the right adherend was 1.8×10^6 psi (12.4 GPa). Orthotropic stiffness values for wood were based on the longitudinal MOE and assigned according to Bodig and Jayne.[36] Poisson's ratios were assigned according to Bodig and Goodman.[37] The geometric and material properties axes were made coincident to further simplify the model. The adhesive layer of the basic model was isotropic with an MOE of 1.0×10^6 psi (6.9 GPa) based on work by Triche and Hunt.[38] The adhesive layer was modeled with three

elements across the 0.004-in. (0.1 mm) thickness and was assumed to be continuous such that no gaps or voids existed. Adhesive stiffness parametric FE models had adhesive MOE values of 0.5, 0.75, 1.0, 1.25, and 1.5×10^6 psi (3.4, 5.2, 6.9, 8.6, and 10.3 GPa).

Glueline Thickness

The parameters for the glueline thickness study were set up to simulate potential glueline thicknesses that might vary as a result of clamping forces during on-line assembly. High compressive on-line forces were represented by the thin gluelines, and low on-line forces were represented by the thicker gluelines. Five parametric models, shown in Figure 2, were constructed with glueline thicknesses ranging from 0.001 in. (0.025 mm to 0.016 in. (0.41 mm)). Tip clearance was also adjusted according to glueline thickness (Fig. 2). The thinner glueline models produced aspect ratios in the critical regions that approached 12: 1, whereas the thicker glueline models had aspect ratios of less than 3: 1.

RESULTS AND DISCUSSION

Results presented in this paper are the result of analytical models; no experimental techniques were employed to verify stresses attained from the various FE models. Analysis of adherend stresses in the adherends was limited to the longitudinal and radial directions because of the orthogonal properties of wood. Accordingly, the relatively isotropic character of adhesives makes it reasonable to analyze the glueline in terms of principal stresses.

Effect of Adhesive Stiffness

Results for longitudinal and radial adherend stress concentrations for varying glueline stiffnesses are summarized in Table I and are shown graphically in Figures 3 and 4. The results show that flexible adhesives promote adherend stress concentrations in both the

TABLE I
The effect of glueline stiffness on structural finger joint maximum longitudinal and radial adherend stresses, maximum shear stress in the adherends and the adhesive, and the maximum principal stress in the adhesive

	Glueline Stiffness ($\times 10^6$ psi)	$\sigma_{x_{max}}$	$\sigma_{y_{max}}$	τ_{max}	$\sigma_{1_{max}}$
Adherends	0.5			0.125	
	0.75			0.088	
	1.0			0.063	
	1.25			0.043	
	1.5			0.043	
Glueline	0.5			0.221	0.91
	0.75			0.162	1.10
	1.0			0.110	1.08
	1.25			0.067	1.12
	1.5			0.058	1.15

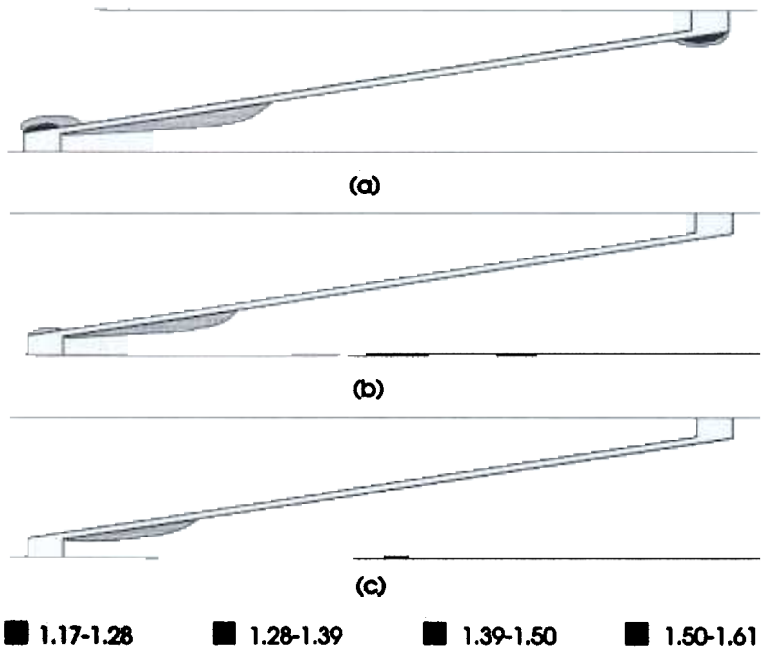

FIGURE 3 Effect of adhesive stiffness on longitudinal adherend stresses along a finger-joint glueline. Loading was in the tensile direction, and stresses were normalized with respect to loading. Longitudinal MOE for the left adherend = 1.4×10^6 psi; right adherend = 1.8×10^6 psi; and adhesive = (a) 0.5×10^6 psi, (b) 1.0×10^6 psi, and (c) 1.5×10^6 psi.

longitudinal and radial directions. The analytical model showed that adherend stresses for finger joints constructed with a flexible adhesive were concentrated at the finger bases, with these stresses being more severe in the flexible adherend (Fig. 3). Radial stresses demonstrated a similar pattern but were concentrated primarily at the base of the stiff adherend (Fig. 4). Longitudinal and radial stresses in the adherends were both reduced to relatively low levels when the adhesive stiffness approached that of the adherends.

Adherend shear stresses in the longitudinal-radial plane were affected by adhesive stiffness, with the largest adherend shear stresses occurring in joints constructed with a flexible adhesive (Fig. 5). The same result of increasing shear stress with decreasing adhesive stiffness was also seen in the adhesive layer. The effect of adhesive stiffness on both adherend and adhesive shear stresses diminished as the adhesive stiffness approached the adherend stiffness. This relationship between adherend shear stresses and adhesive stiffness suggests that the efficiency of the adhesive in transmitting axial stresses among adherends is a function of adhesive stiffness.

Reduced uniaxial stresses in the adherends for increasing adhesive stiffnesses were balanced by increased stress levels in the adhesive, as shown in Figure 6. Increased adhesive stiffness increased the magnitude of principal stresses in the adhesive (Table I) as well as distributing the stresses over a large area. A relatively flexible adhesive leads to low stress levels localized near the base of the flexible fingers, whereas a stiff adhesive

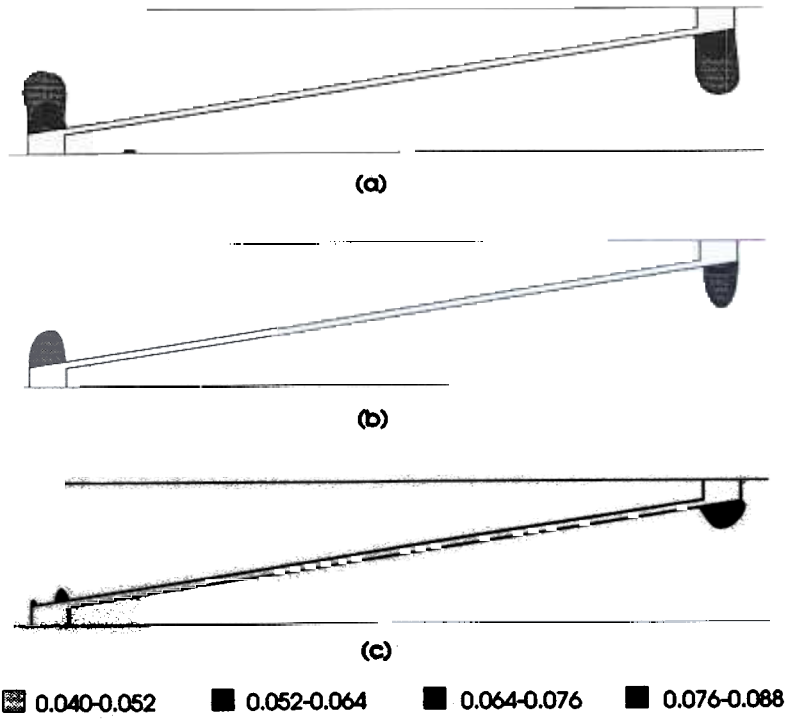

FIGURE 4 Effect of adhesive stiffness on radial adherend stresses along a finger-joint glueline. Loading was in the tensile direction, and stresses were normalized with respect to loading. Longitudinal MOE for the left adherend = 1.4×10^6 psi; right adherend = 1.8×10^6 psi; and adhesive = (a) 0.5×10^6 psi, (b) 1.0×10^6 psi, and (c) 1.5×10^6 psi.

promotes large principal stresses in the adhesive distributed throughout the entire adhesive layer.

Effect of Adhesive Thickness

Table II shows that longitudinal adherend stresses are minimally affected by the thickness of the adhesive layer (Figure 7). Thin and thick adhesive layers concentrate longitudinal stresses at the base of the flexible adherend. However, the greatest longitudinal adherend stresses concentrate at the tip of the stiffer finger for thin and thick adhesive layers. Table II shows a slight increase in the maximum longitudinal adherened stress concentration for the thick adhesive layer. This increase appears to be due to an interaction of longitudinal stresses in the finger tip and base of the stiff adherend (Fig. 7c), which results in an accumulation of longitudinal stresses at the finger tip and base of the stiff adherend.

The effect of glueline thickness is similar to that of adhesive stiffness; stresses are concentrated at the base of the fingers, and radial adherend stresses decrease with thinner adhesive layers (Fig. 8). The adherend radial stresses from the thin to the thick adhesive layer decreased by 22 percent, which was comparable with the 26-percent

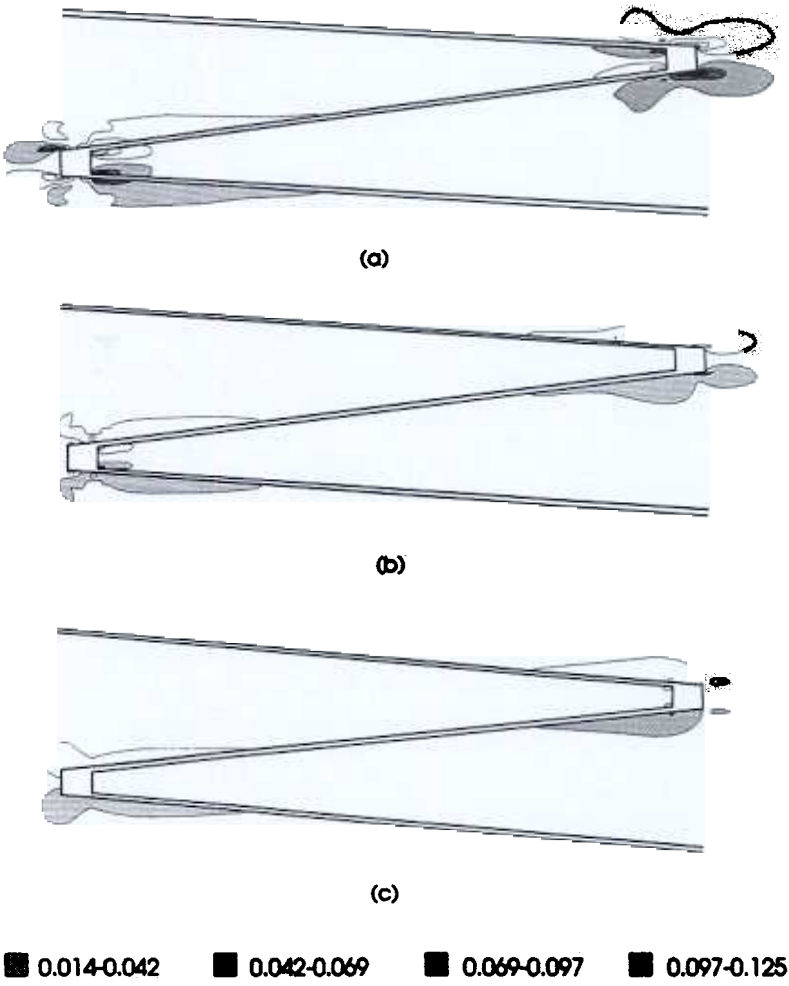

FIGURE 5 Effect of adhesive stiffness on shear adherend stresses along a finger-joint glueline. Loading was in the tensile direction, and stresses were normalized with respect to loading. Longitudinal MOE for the left adherend = 1.4×10^6 psi; right adherend = 1.8×10^6 psi; and adhesive = (a) 0.5×10^5 psi, (b) 1.0×10^6 psi, and (c) 1.5×10^6 psi. Positive shear values are shown as shaded contours, negative shear values shown as unshaded contours.

decrease from the flexible to the stiff adhesive. The largest decrease in adherend radial stresses occurred from 0.001 in. (0.025 mm) to 0.004 in. (0.10 mm), with little change from 0.004 in. (0.01 mm) to 0.016 in. (0.41 mm).

Thicker adhesive layers do seem to exhibit greater shear stresses (Fig. 9), both in the adherends and the adhesive. However, Table II shows that this effect of adhesive thickness on adherend and adhesive shear stress distributions was substantially less than the effect of adhesive stiffness. The increase in shear stress levels for the thicker adhesives is caused by the transmittance of stresses among adherends across an

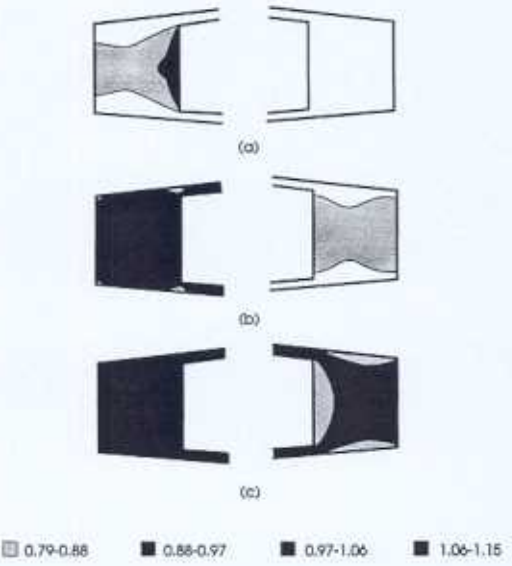

FIGURE 6 Effect of adhesive stiffness on principal adhesive stresses at the left and right tip of each finger along a finger-joint glueline. Loading was in the tensile direction, and stresses were normalized with respect to loading. Longitudinal MOE for the left adherend = 1.4×10^6 psi; right adherend = 1.8×10^6 psi; and adhesive = (a) 0.5×10^6 psi, (b) 1.0×10^6 psi, and (c) 1.5×10^6 psi.

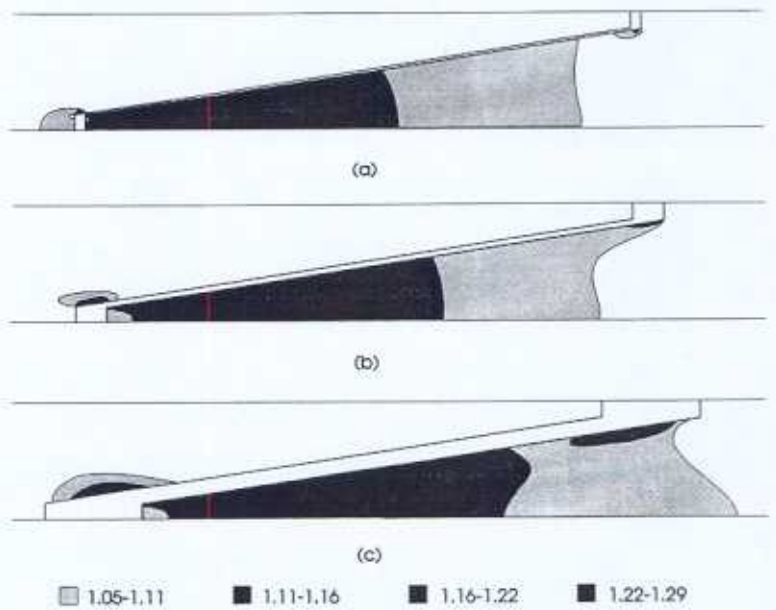

FIGURE 7 Effect of glueline thickness on longitudinal adherend stresses along a finger-joint glueline. Loading was in the tensile direction, and stresses were normalized with respect to loading. Longitudinal MOE for the left adherend = 1.4×10^6 psi; right adherend = 1.8×10^6 psi; and adhesive = 1.0×10^6 psi. Glueline thickness = (a) 0.001 in.; (b) 0.004 in.; and (c) 0.016 in.

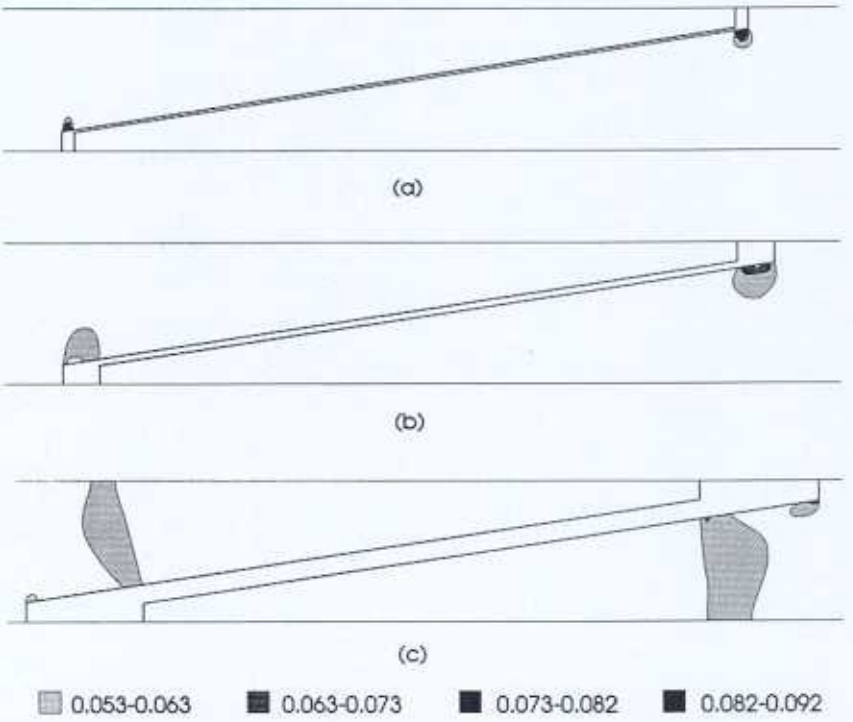

FIGURE 8 Effect of glueline thickness on radial adherend stresses along a finger-joint glueline. Loading was in the tensile direction, and stresses were normalized with respect to loading. Longitudinal MOE for the left adherend = 1.4×10^6 psi; right adherend = 1.8×10^6 psi; and adhesive = 1.0×10^6 psi. Glueline thickness = (a) 0.001 in.; (b) 0.004 in.; and (c) 0.016 in.

TABLE II
The effect of glueline thickness on structural finger joint maximum longitudinal and radial adherend stresses, maximum shear stress in the adherends and the adhesive, and the maximum principal stress in the adhesive

	Glueline Thickness (in.)	$\sigma_{x_{max}}$	$\sigma_{y_{max}}$	τ_{max}	$\sigma_{1_{max}}$
Adherends	.001	1.26	0.092	0.056	
	.002	1.27	0.080	0.053	
	.004	1.26	0.074	0.063	
	.008	1.25	0.071	0.074	
	.016	1.29	0.072	0.076	
Glueline	.001			0.105	1.11
	.002			0.106	1.10
	.004			0.110	1.08
	.008			0.117	1.06
	.016			0.151	1.07

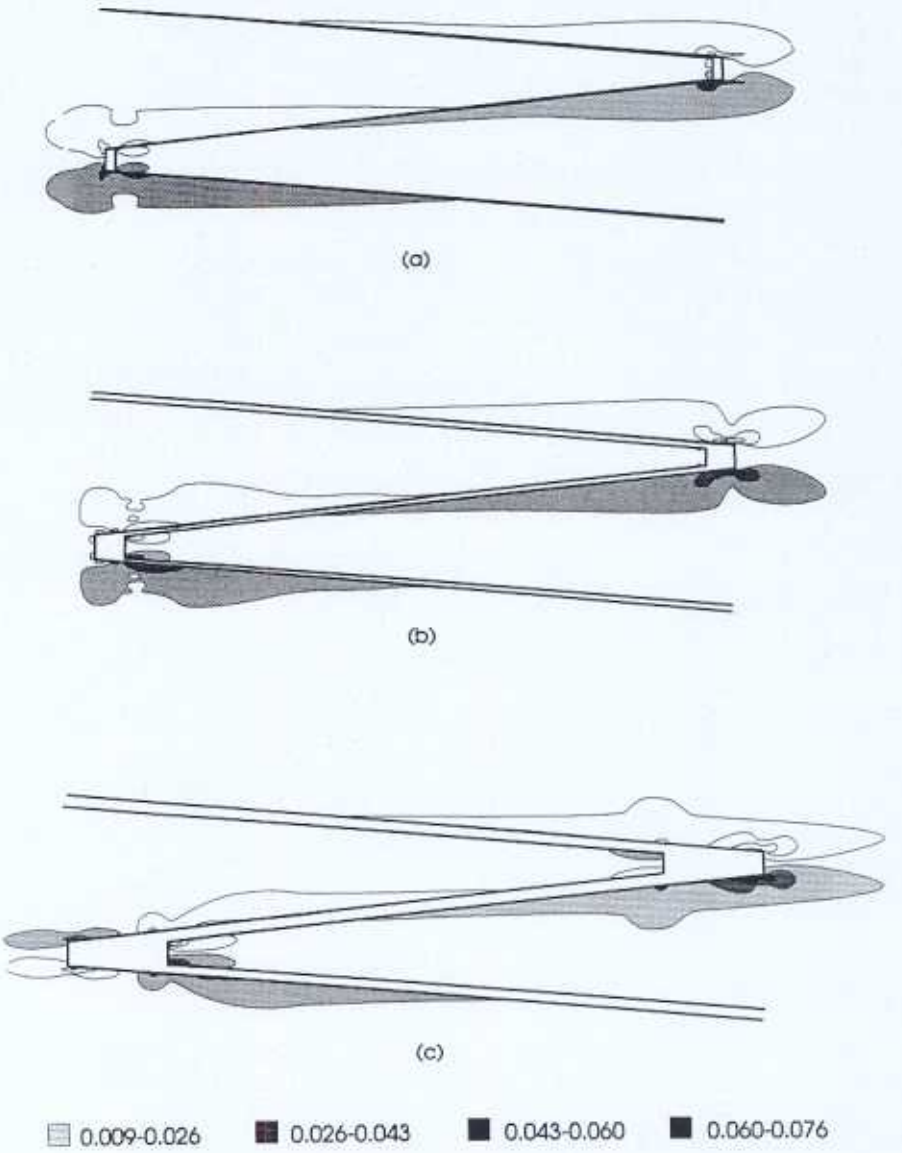

FIGURE 9 Effect of glueline thickness on shear adherend stresses along a finger-joint glueline. Loading was in the tensile direction, and stresses were normalized with respect to loading. Longitudinal MOE for the left adherend = 1.4×10^6 psi; right adherend = 1.8×10^6 psi; and adhesive = 1.0×10^6 psi. Glueline thickness = (a) 0.001 in.; (b) 0.004 in.; and (c) 0.016 in. Positive shear values are shown as shaded contours, negative shear values shown as unshaded contours.

increasing adhesive interface that is less elastic than the adherends that it joins. Thus, shear stresses can be kept to a minimum primarily by maintaining the thinnest practical adhesive layer and, secondarily, by using an adhesive that is comparable in stiffness with the adherends to be joined.

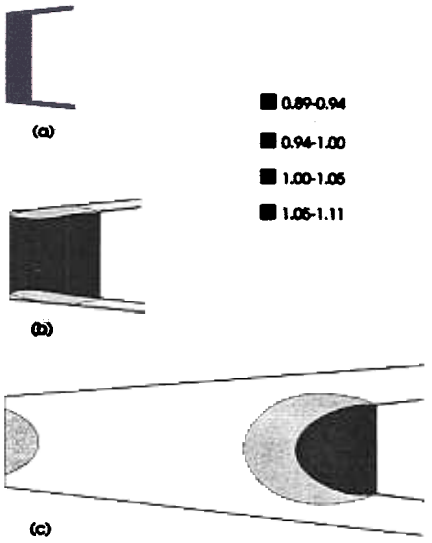

FIGURE 10 Effect of glueline thickness on principal adhesive stresses at the fingertip of the right adherend. Loading was in the tensile direction, and stresses were normalized with respect to loading. Longitudinal MOE for the left adherend = 1.4×10^6 psi; right adherend = 1.8×10^6 psi; and adhesive = 1.0×10^6 psi. Glueline thickness = (a) 0.001 in.; (b) 0.004 in.; and (c) 0.016 in.

Figure 10 depicts the principal adhesive stress distribution patterns at the tip of the stiff adherend and shows that the glueline thickness has only a minor effect on the principal adhesive stresses. Not only do the principal adhesive stress distribution patterns remain unaffected by the adhesive thickness, but the magnitude seems unaffected as well (Table II).

CONCLUSIONS

Adhesive stiffness and thickness have a significant effect on how stresses are transferred among adherends. A stiff adhesive is recommended to reduce longitudinal and radial stress concentrations at the finger base. In addition, a stiff adhesive dramatically reduces the shear stress levels within the adhesive layer. However, this reduction in adhesive shear stress may be offset by an increase in principal adhesive stresses.

Another recommendation is to maintain compressive on-line forces great enough to ensure a relatively thin glueline while minimizing splitting of the adherends at the finger base. Although a thin adhesive layer does develop radial adherend stress concentrations, these concentrations are negated by large adhesive shear stresses that form in thick gluelines, the result of poor axial stress transmittance.

The models used in this study were based on linear finite elements and assumed material homogeneity. These simplistic assumptions were made to reduce the complexity of the model and to provide fundamental information about the mechanisms of

stress transfer among adherends. More accurate models are needed that incorporate the nonlinear behavior of wood as well as growth-related nonhomogeneities such as growth rings and localized grain deviations. The stiffness of the adhesive layer in these models was less than the stiffness of the adherends; caution should be taken when extrapolating conclusions on systems with substantially stiffer adhesives or more flexible adherends.

References

1. United States Department of Agriculture. *1986 Yearbook of Agriculture: Research for Tomorrow* (U.S. Department of Agriculture, Washington, DC, 1986).
2. E. C. O. Erickson. *Strength Tests of Spliced Studs* (USDA Forest Service, Forest Products Laboratory, Madison, WI, 1941). Research Report FPL 1275.
3. R. F. Luxford and R. H. Krone. *End Joints of Various Types in Douglas-fir and White Oak Compared for Strength* (USDA Forest Service, Forest Products Laboratory, Madison, WI, 1946). Research Report No. 1622.
4. R. C. Moody and B. Bohannan. *Flexural Properties of Glued-Laminated Southern Pipe Beams—Finger Joint and Specific Gravity Effects* (USDA Forest Service, Forest Products Laboratory, Madison, WI, 1971). Research Paper FPL 151.
5. D. B. Richards and F. E. Goodrick, *Forest Prod. J.* 9(6), 177–179 (1959).
6. M. L. Selbo, *Test for Quality of Glue Bonds in End-Jointed Lumber* (USDA Forest Service, Forest Products Laboratory, Madison, WI, 1962). Research Report No. 2258.
7. M. L. Selbo, *Forest Prod. J.* 13(9), 390–400 (1963).
8. J. Jung, *Forest Prod. J.* 34(5), 51–55 (1984).
9. B. Bohannan and K. Kanvik. *Fatigue Strength of Finger Joints* (USDA Forest Service, Forest Products Laboratory, Madison, WI, 1969). Research Paper FPL 114.
10. N. P. Kutscha and R. W. Caster, *Forest Prod. J.* 37(4), 43–48 (1987).
11. H. Miyajima and H. Ikuta, *Res. Bull. Collect Exp. Forest* (Hokkaido University) 33(1), 167–200 (1975).
12. M. Mori and T. Hoshi, *Wood Ind.* (Tokyo) 18(3), 123–129 (1963).
13. D. B. Richards, *Forest Prod. J.* 13(6), 250–251 (1963).
14. F. Erdogan and M. Ratwani, *J. Comp. Mat.* 5, 378–393 (1971).
15. T. Sawa, Y. Nakano, and K. Temma, *J. Adhesion* 24, 245–258 (1987).
16. F. W. Smith and D. T. Penney, *Forest Prod. J.* 12(4), 227–235 (1980).
17. D. Chen and S. Cheng, *ASME J. Appl. Mech.* 50, 109–115 (1983).
18. D. Chen and S. Cheng, *ASME J. Appl. Mech.* 57, 78–83 (1990).
19. J. N. Reddy and S. Roy. *Finite-Element Analysis of Adhesively Bonded Joints* (U.S. Department of Commerce, National Technical Information Service, Washington, DC, 1985). Catalog Number PB86-100708.
20. H. L. Groth and I. Brottare, *ASTM J. Test. and Eval.* 17(2), 131–134 (1989).
21. D. W. Schmueser, N. L. Johnson, and R. T. Foister, *J. Adhesion* 24, 47–64 (1987).
22. T. M. Roberts, *J. Eng. Mech.* 115(11), 2460–2479 (1987).
23. S. Amijima and T. Fujii, *Int. J. Adhesion and Adhesives* 7(4), 199–204 (1987).
24. B. Dattaguru, R. A. Everett Jr., J. D. Whitcomb, and W. S. Johnson, *J. Eng. Mater. Technol. Trans. ASME* 106, 59–65 (1984).
25. C. T. Herakovich, A. Nagarkar, and D. A. O'Brian, *Modern Development in Composite Materials and Structures* (ASME-Aerospace Division, New York, 1979), pp. 53–66.
26. W. S. Johnson, *ASTM J. Test and Eval.* 15(6), 303–324 (1987).
27. S. Aicher and W. Klöck, *Bauen mit Holz* 5, 356–362 (1990).
28. S. Aicher and W. Klöck, in *Proceedings, 1991 International Timber Engineering Conference, London, England* (Timber Research and Development Association, High Wycombe, England, September 2–5, 1991), pp. 3.66–3.76.
29. P. Pellicane, *Forest Prod. J.* 42(1), 50–52 (1992).
30. R. J. Leichti, in *Proceedings, 1988 International Conference on Timber Engineering, Vol. 1* (Madison, WI, Forest Products Research Society, 1988), pp. 647–653.
31. L. H. Groom and R. J. Leichti, in *Technical Forum Presentation Abstracts* (New Orleans, LA, FPRS Annual Meeting, June, 1991), pp. 75.

32. R. J. Leichti and L. H. Groom, *Proceedings, Adhesives and Bonded Wood Products Symposium* (Seattle, WA, October 1991), In press.
33. H. R. Milner and E. Yeoh, *J. Struct. Eng.* 117(3), 755–766 (1991).
34. H. R. Milner, T. Song, and E. H. Yeoh, in *Proceedings of the Second Pacific Timber Engineering Conference, Auckland, New Zealand, August 28–31, 1989, Vol 2* (University of Auckland, New Zealand, Centre for Continuing Education, 1989), pp. 159–164.
35. P. J. Pellicane and R. C. Moody, in *Proceedings, 1988 International Conference on Timber Engineering, Seattle, WA, September 19–22, 1988, Vol. 1* (Madison, WI, Forest Products Research Society, 1988), pp. 899–908.
36. J. Bodig and B. A. Jayne, *Mechanics of Wood and Wood Composites* (Van Nostrand Reinhold Company, New York, 1982).
37. J. Bodig and J. R. Godman, *Wood Sci.* 5(4), 249–264 (1973).
38. M. Triche and M. O. Hunt, *Forest Prod. J.* 43(11/12), 33–44 (1993).